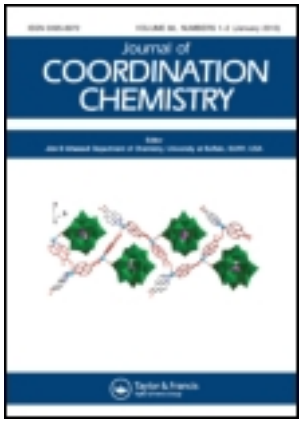

Journal of Coordination Chemistry
Publication details, including instructions for authors and subscription information:
http://www.tandfonline.com/loi/gcoo20

Synthesis, characterization, catalytic, and biological studies of macrobicyclic binuclear nickel(II) complexes of 1,8-difunctionalized cyclam derivatives

R. Prabu [a] , A. Vijayaraj [a] , R. Suresh [a] , R. Senbhagaraman [b] , V. Kaviyarasan [b] & V. Narayanan [a]

[a] Department of Inorganic Chemistry, School of Chemical Sciences , University of Madras , Chennai , India

[b] Center for Advanced Studies in Botany , University of Madras , Chennai , India

Accepted author version posted online: 19 Nov 2012.Published online: 19 Dec 2012.

To cite this article: R. Prabu , A. Vijayaraj , R. Suresh , R. Senbhagaraman , V. Kaviyarasan & V. Narayanan (2013) Synthesis, characterization, catalytic, and biological studies of macrobicyclic binuclear nickel(II) complexes of 1,8-difunctionalized cyclam derivatives, Journal of Coordination Chemistry, 66:2, 206-217, DOI: 10.1080/00958972.2012.751488

To link to this article: http://dx.doi.org/10.1080/00958972.2012.751488

Journal of Coordination Chemistry
Vol. 66, No. 2, 20 January 2013, 206–217

Synthesis, characterization, catalytic, and biological studies of macrobicyclic binuclear nickel(II) complexes of 1,8-difunctionalized cyclam derivatives

R. PRABU†§, A. VIJAYARAJ†, R. SURESH†, R. SENBHAGARAMAN‡
V. KAVIYARASAN‡ and V. NARAYANAN†*

†Department of Inorganic Chemistry, School of Chemical Sciences, University of Madras, Chennai, India; ‡Center for Advanced Studies in Botany, University of Madras, Chennai, India

(*Received 12 January 2012; in final form 4 October 2012*)

New Schiff base binuclear nickel(II) complexes of N-substituted cyclam derivatives have been prepared by template condensation of 1,8-[bis(3-formyl-2-hydroxy-5-bromo)benzyl]-l,4,8,11-tetraaza-cyclo-tetradecane (PC) with appropriate aliphatic diamines and nickel(II) perchlorate. The ligand possesses two coordination sites, an N_4O_2 amine compartment and N_3O_2/N_4O_2 imine compartment. The structural features of the complexes have been confirmed by elemental analysis, IR, UV–Vis, and mass spectra. From the data, octahedral geometry around the two nickels has been suggested. The electrochemical behavior of the complexes show two irreversible one-electron reduction process in the cathodic region and show two irreversible one-electron oxidation process at the anode. Hydrolysis of 4-nitrophenylphosphate using the complexes as catalysts have been carried out. Antimicrobial screening data show good results. The binding of the complexes to calf thymus DNA (CT DNA) has been investigated with absorption and emission spectroscopy. Ni_2L^1 displays significant cleavage of circular plasmid pBR322 DNA to linear form. Spectral, electrochemical, and catalytic studies support distortion of the nickel geometry that arises as the macrocyclic ring size increases.

Keywords: Cyclam; Binuclear Ni(II) complexes; Cyclic voltammetry; Antimicrobial activity; DNA binding and cleavage studies

1. Introduction

Synthesis of macrocyclic ligands that can give dinuclear metal complexes with interactions between metal centers, especially phenol-based compartmental ligands, have important applications [1–4]. Functionalized tetraazacycloalkanes have been widely studied, due to their ability to chelate a wide variety of metal cations [5]. N-functionalization of 14-membered saturated tetraazamacrocycles, such as 1,4,8,11-tetraazacyclododecane (cyclam), has been the subject of intense investigation, mainly due to their use as MRI contrast agents [6] and radiodiagnostic and radiotherapeutic agents [7]. Applications require fine tuning of the chelating properties of the ligand derivative by changing the nature, number, and

*Corresponding author. Email: vnnara@unom.ac.in
§Present address: Department of Chemistry, Karpaga Vinayaka College of Engineering and Technology, Kancheepuram, India

ISSN 0095-8972 print/ISSN 1029-0389 online
http://dx.doi.org/10.1080/00958972.2012.751488

relative positions of the functional groups. Selective difunctionalization of cyclam is difficult to achieve. Transition metal compounds containing Schiff base ligands have been of interest for many years [8], playing an important role in coordination chemistry related to catalysis, enzymatic reactions, magnetism, and molecular architectures [9].

Six-coordinate dinuclear Ni(II) complexes are active catalysts for phosphate hydrolysis. Many nickel(II) complexes have been synthesized and their interactions with DNA have been studied [10–14]. Compared with the number of studies dealing with mononuclear complexes, relatively few studies on binuclear complexes [15, 16] have been reported to date. Recently, we reported catalytic and biological activities of macrocyclic binuclear Ni (II) analogs [17]. Here, we report new template Schiff base condensation of dicarbonyl compounds with aliphatic diamines and fine tuning of the macrocyclic structure for precise coordination requirements of the metal ion. The macrocyclic ring has two compartments, one N_4O_2 donor and the other N_3O_2/N_4O_2 donors. Spectral, magnetic, electrochemical, catalytic, antimicrobial, and DNA binding of the complexes are discussed.

2. Experimental

2.1. *Analytical and physical measurements*

C, H, and N elemental analyses were performed on a Haereus CHN rapid analyzer. Nickel analysis was carried out on a Varian Atomic 76 Absorption spectrophotometer. ^{1}H NMR spectra were recorded with a Bruker 300 MHz FT–NMR spectrometer using TMS as an internal standard in $CDCl_3$. FT-IR spectra were obtained using a Perkin Elmer FT-IR spectrometer using KBr disks. The UV–Vis spectra of complexes were recorded using a Perkin Elmer Lambda 35 spectrophotometer from 200 to 1100 nm. Electron spray ionization mass spectral measurements were made using a Thermo Finnigan LCQ-6000 advantage Max-ESI mass spectrometer. Electrochemical measurements were recorded on a CHI-600A electrochemical analyzer using a three electrode set-up of a glassy carbon working, platinum wire auxiliary, and an Ag/AgCl reference electrode under oxygen-free conditions. A ferrocene/ferrocenium (1^+) couple was used as an internal standard and $E_{1/2}$ of the ferrocene/ferrocenium (Fc/Fc^+) couple under the experimental condition is 470 mV. TBAP was used as a supporting electrolyte. Molar conductances (Λ_m) were measured using an Elico digital conductivity bridge, model CM-88, using freshly prepared solution of the complex in acetonitrile.

2.2. *Chemicals and reagents*

3-Chloromethyl-5-bromo salicylaldehyde [18], 1,4,8,11-tetraazatricyclo[9.3.1.1$^{[4,8]}$]-hexadecane [19], and 1,8-[bis(3-formyl-2-hydroxy-5-bromo)-benzyl]-4,11-diazaniatricyclo [9.3.1.1$^{[4,8]}$] hexadecane dichloride [20] were prepared following the reported procedure. Analytical grade methanol, acetonitrile, and dimethylformamide were purchased from Qualigens and used as received. TBAP, as supporting electrolyte in electrochemical measurements, was purchased from Fluka and recrystallized from hot methanol. (Caution! TBAP is potentially explosive and hence, care should be taken.) All other reagents were obtained from standard commercial sources and used without purification.

2.3. *Antimicrobial assay*

All microorganisms were incubated at 37 °C for 24 h in Nutrient broth and *Candida albicans* in Sabouraud dextrose broth at 37 °C for 48 h. For investigation of antibacterial and antifungal activity, metal complexes were dissolved in DMSO to a final concentration of 100 μg mL^{-1}. Each sample was filled into the wells of agar plates directly. Plates swabbed with the bacteria culture were incubated at 37 °C for 48 h and the fungi were incubated at 37 °C for 24 h. At the end of the incubation period, inhibition zones formed on the media were evaluated in mm. Studies were performed in duplicate and the inhibition zones were compared with those of reference disks. Inhibitory activity of DMSO was also tested. Reference values used from reference disk as a control were as follows: Tetracycline (30 μg) and Ampicillin (10 μg). All determinations were done in triplicate.

2.4. *DNA binding experiment*

The concentration of CT DNA per nucleotide was measured by using its extinction coefficient at 260 nm (6600 $M^{-1}cm^{-1}$). The absorbances at 260 nm (A_{260}) and at 280 nm (A_{280}) for CT DNA were measured to check purity [21]. The ratio A_{260}/A_{280} was 1.84, indicating that CT DNA was satisfactorily free from protein. Buffer [50 mM tris(hydroxymethyl)aminomethane, tris, pH 7.2, 1 mM NaCl] was used for the absorption studies. Absorption titration experiments were carried out by varying the DNA concentration (0–60 μM) and maintaining the metal-complex concentration constant (30 μM). While measuring absorption spectra, an equal amount of DNA was added to both the compound solution and the reference solution to eliminate the absorbance of DNA itself. Absorption spectra were recorded after each successive addition of DNA and equilibration (approximately, 5 min).

By the fluorescence spectral method, relative binding of complexes to CT–DNA were studied with an EB-bound CT–DNA solution in Tris–HCl/NaCl buffer, pH 7.5. A 2 mL solution of 20 μM DNA and 0.33 μM of EB (at saturation binding level) was titrated by 0–40 μM metal complexes ($\lambda_{max} = 500$ nm, $\lambda_{max} = 520$–800 nm).

The DNA cleavage experiments were done by agarose gel electrophoresis, which was performed by incubation at 37 °C as follows: pBR322 DNA (0.5 μg) in 50 mM Tris–HCl/1 mM NaCl buffer (pH 7.5) was treated with $[Ni_2L^1]$ in the absence of additives.

2.5. *Synthesis of precursor compound*

1,8-[Bis(3-formyl-2-hydroxy-5-bromo)-benzyl]-l,4,8,11-tetraazacyclotetradecane. The precursor compound was synthesized by hydrolysis of 1,8-[bis(3-formyl-2-hydroxy-5-bromo)-benzyl]-4,11-diazaniatricyclo[9.3.1.1$^{[4,8]}$]hexadecane dichloride according to the reported procedure [22].

2.6. *Synthesis of the binuclear nickel(II) complexes*

2.6.1. $[Ni_2L^1(ClO_4)](ClO_4)$. The complexes were prepared by a general synthetic method in which methanolic solution of nickel(II) perchlorate hexahydrate (0.74 g, 0.002 M) was added to a hot solution of precursor (1.00 g, 0.002 M) in methanol; this was

followed by addition of a methanolic solution (diethylenetriamine (0.21 g, 0.002 M) and triethylamine (0.41 g, 0.004 M)). After refluxing an hour, another equivalent of nickel(II) perchlorate (0.74 g, 0.002 M) was added and the reaction mixture was refluxed for 24 h. The resulting solution was filtered hot and allowed to stand at room temperature. After slow evaporation of the solvent at 25 °C, dark green compound was collected by filtration, washed with diethyl ether, recrystallized in acetonitrile, and dried in vacuum.

Yield: 0.90 g (55%). Anal. Calcd for $C_{30}H_{41}N_7O_{10}Ni_2Cl_2Br_2$ (%): C: 35.75, H: 4.10, N: 9.73, Ni: 11.65. Found (%): C: 35.68, H: 4.15, N: 9.76, Ni: 11.57. ESI mass (m/z): $[Ni_2L^1(ClO_4)–ClO_4]^+$: 907.51. Conductance (Λ_m, S cm^2 M^{-1}): 164. Selected IR data (KBr disk) (ν cm^1): 3249 ν (NH), 1628 ν (C=N), 1542 (phenoxide bridge) [1102, 1095, and 1087 coordinated ClO_4^-], 626 (ClO_4^-).

$[Ni_2L^2](ClO_4)_2$, $[Ni_2L^3](ClO_4)_2$, $[Ni_2L^4](ClO_4)_2$, and $[Ni_2L^5](ClO_4)_2$ were synthesized by following the above procedure using triethylenetetramine (0.29 g, 0.002 M), *N,N′*-bis-(3-aminopropyl)ethylenediamine (0.35 g, 0.002 M), *N,N′*-bis-(3-(3-aminopropyl)propyl-enediamine (0.38 g, 0.002 M), or *N,N′*-bis-(3-aminopropyl)piperazine (0.40 g, 0.002 M) respectively, instead of diethylenetriamine.

2.6.2. $[Ni_2L^2](ClO_4)_2$. *Dark green. Yield*: 0.98 g (60%). Anal. Calcd for $C_{32}H_{46}N_8O_{10}$-$Ni_2Cl_2Br_2$ (%): C: 36.57, H: 4.41, N: 10.66, Ni: 11.17. Found (%): C: 36.50, H: 4.48, N: 10.58, Ni: 11.10. ESI mass (m/z): $[Ni_2L^2–2ClO_4]^{2+}$: 376.01. Conductance (Λ_m, S cm^2 M^{-1}): 209. Selected IR data (KBr disk) (ν/cm^{-1}): 3250 ν (NH), 1630 ν (C=N), 1550 (phenoxide bridge), 1088 (s, uncoordinated ClO_4^-), and 624 ν (ClO_4^-).

2.6.3. $[Ni_2L^3]$ $(ClO_4)_2$. *Dark green. Yield*: 0.91 g (56%). Anal. Calcd for $C_{34}H_{50}N_8O_{10}$-$Ni_2Cl_2Br_2$ (%): C: 37.85, H: 4.67, N: 10.39, Ni: 10.88. Found (%): C: 45.60, H: 5.94, N: 11.95, Ni: 12.69. ESI mass (m/z): $[Ni_2L^3–2ClO_4]^{2+}$: 389.85. Conductance (Λ_m, S cm^2 M^{-1}): 210. Selected IR data (KBr disk) (ν/cm^{-1}): 3273 ν (NH), 1639 ν (C=N), 1558 (phenoxide bridge), 1099 (s, uncoordinated ClO_4^-), and 625 ν (ClO_4^-).

2.6.4. $[Ni_2L^4](ClO_4)_2$. *Dark green. Yield*: 1.05 g (61%). Anal. Calcd for $C_{35}H_{52}N_8O_{10}$-$Ni_2Cl_2Br_2$ (%): C: 38.46, H: 4.80, N: 10.25, Ni: 10.74. Found (%): C: 38.40, H: 4.72, N: 10.31, Ni: 10.80. ESI mass (m/z): $[Ni_2L^4–2ClO_4]^{2+}$: 396.12. Conductance (Λ_m, S cm^2 M^{-1}): 220. Selected IR data (KBr disk) (νr2/cm^{-1}): 3310 ν (NH), 1631 ν (C=N), 1549 (phenoxide bridge), 1093 (s, uncoordinated ClO_4^-), and 626 ν (ClO_4^-).

2.6.5. $[Ni_2L^5](ClO_4)_2$. *Dark green. Yield*: 1.12 g (64%). Anal. Calcd for $C_{36.}H_{52}N_8O_{10}$-$Ni_2Cl_2Br_2$ (%): C: 39.13, H: 4.74, N: 10.14, Ni: 10.62. Found (%): C: 46.96, H: 6.08, N: 11.50, Ni: 12.25. ESI mass (m/z): $[Ni_2L^5–2ClO_4)]^{2+}$: 402.95. Conductance (Λ_m, S cm^2 M^{-1}): 228. Selected IR data (KBr disk) (ν/cm^{-1}): 3332 ν (NH), 1646 ν (C=N), 1549 (phenoxide bridge), 1095 (s, uncoordinated ClO_4^-), and 625 ν (ClO_4^-).

3. Results and discussion

Using the template method, five macrobicyclic binuclear nickel(II) complexes were prepared by Schiff base condensation of the precursor compound with aliphatic diamines in the presence of the metal salt. The synthetic pathway is shown in scheme 1. Previous

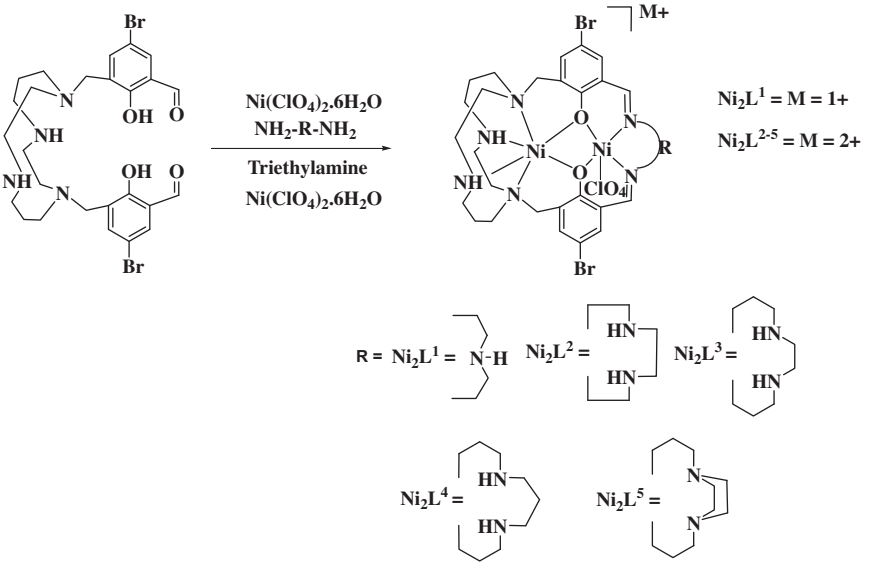

Scheme 1. Synthesis of binuclear Ni(II) complexes.

studies [17] discuss structural properties and similar binuclear nickel(II) complexes. Conductance value was 164 S cm^2 M^{-1} for Ni_2L^1, suggesting a 1 : 1 electrolyte. Conductance values of Ni_2L^{2-5} (Λ_m, 209–228 S cm^2 M^{-1}) show 1 : 2 electrolytes [23]. Hence, it is proposed that one nickel(II) in the amine compartment is six coordinate and the other in the imine compartment is five/six coordinate. Spectral, electrochemical, catalytic, and biological studies of the complexes were carried out.

3.1. *Spectral studies*

Infrared spectra for the complexes show a band at 3249–3332 cm^{-1}, indicating the presence of –NH in the complexes. All the complexes show a sharp band at 1630–1650 cm^{-1} due to –C=N [24]. This shows that the aldehydes are completely converted into imine groups by disappearance of the aldehydic –C=O stretch at 1680 cm^{-1}. All binuclear nickel (II) complexes show two sharp peaks at 1100 and 624 cm^{-1}, assigned to perchlorate [25]. Ni_2L^1 shows splitting of the peak at 1100 cm^{-1} together with a band at 628 cm^{-1}. Splitting suggests coordinated perchlorate; in Ni_2L^{2-5}, the perchlorate 1100 cm^{-1} absorption does not show any splitting [26], indicating the presence of an uncoordinated perchlorate. New bands at 1530–1560 cm^{-1} indicate that all the complexes have phenoxide bridges [27]. The FT-IR spectrum of a complex is shown in Supplementary Material.

Electronic absorption spectra for the complexes were recorded at room temperature using DMF and the data are tabulated in table 1. Bands below 312 nm are attributed to intra-molecular (π–π^*). An intense peak at 380–430 nm is due to ligand-to-metal charge transfer transition, while weaker bands at 550–1060 nm are attributed to d–d transitions, characteristic of Ni^{2+} with 5/6 coordination [28]. Absorption spectra of binuclear Ni(II) complexes are similar to octahedral coordinated nickel(II). Bands are assigned as $^3T_{2g}(F) \leftarrow {}^3A_{2g}$, $^3T_{1g}(F) \leftarrow {}^3A_{2g}$, and $^3T_{1g}(P) \leftarrow {}^3A_{2g}$ transitions arising from the $^3A_{2g}$ ground state of an octahedral d^8 ion [29].

Table 1. Electronic spectral data of binuclear nickel(II) complexes.

S. No.	Complexes	λ_{max}, nm (ε, $M^{-1}\,cm^{-1}$)	
		d–d	Charge transfer
1	$[Ni_2L^1(ClO_4)](ClO_4)$	991 (87), 704 (98), 610 (308)	384 (13,302), 270 (15,400)
2	$[Ni_2L^2](ClO_4)_2$	1018 (79), 749 (100), 614 (356)	389 (12,525), 274 (15,795)
3	$[Ni_2L^3](ClO_4)_2$	1020 (86), 771 (89), 620 (306)	392 (13,220), 279 (16,458)
4	$[Ni_2L^4](ClO_4)_2$	1027 (69), 784 (91), 623 (292)	398 (13,750), 284 (16,620)
5	$[Ni_2L^5](ClO_4)_2$	1058 (72), 793 (96), 626 (318)	423 (14,820), 291 (17,925)

3.2. *Electrochemical properties of the complexes*

Electrochemical properties of the complexes were studied by cyclic voltammetry in DMF containing 10^{-1} M tetra(*n*-butyl)ammonium perchlorate (table 2). All the nickel(II) complexes undergo reduction and oxidation in cathodic and anodic potentials, respectively.

3.2.1. Reduction at cathodic potential. The cyclic voltammograms of the complexes from 0 to −1.80 V show two irreversible reduction waves in the cathodic potential region. Controlled potential electrolysis was also carried out and each couple corresponds to a one-electron transfer. The two reduction processes are assigned as follows:

$$Ni^{II}Ni^{II} \rightarrow Ni^{II}Ni^{I} \rightarrow Ni^{I}Ni^{I}$$

The first reduction potential from −0.61 to −0.78 V is ascribed to the metal in the imine compartment (N_3O_2/N_4O_2) while the second reduction potential at −1.30 to −1.46 V is assigned to the metal in the "cyclam" compartment (N_4O_2). The first and second reduction potentials shift anodically as the chelate ring size increases from diethylenetriamine to piperazine linkage. The increase in the chelate ring size increases the macrocyclic ring size and the macrocycles incorporate more flexibility.

3.2.2. Oxidation at anodic potential. All nickel(II) complexes show two oxidation processes from 0.60 to 1.80 V (table 2). The oxidation is irreversible. Controlled potential electrolysis experiment indicates that the two oxidation peaks are associated with stepwise oxidation at nickel(II).

$$Ni^{II}Ni^{II} \rightarrow Ni^{II}Ni^{III} \rightarrow Ni^{III}Ni^{III}$$

Table 2. Electrochemical and hydrolysis data of 4-nitrophenylphosphate.

S. No.	Complexes	Reduction (at cathodic)		Oxidation (at anodic)		Rate constant (k) ($\times 10^{-3}$) min^{-1}
		E^1_{pc}(V)	E^2_{pc}(V)	E^1_{pc}(V)	E^2_{pc}(V)	
1	$[Ni_2L^1(ClO_4)](ClO_4)$	−0.78	−1.46	0.82	1.45	6.35
2	$[Ni_2L^2](ClO_4)_2$	−0.73	−1.41	0.88	1.55	7.98
3	$[Ni_2L^3](ClO_4)_2$	−0.69	−1.38	0.92	1.67	8.74
4	$[Ni_2L^4](ClO_4)_2$	−0.65	−1.34	0.96	1.72	9.26
5	$[Ni_2L^5](ClO_4)_2$	−0.61	−1.30	0.99	1.75	9.84

The first and second oxidation potentials of Ni_2L^1 and Ni_2L^{2-5} shift to more positive value from 0.82 to 0.99 V and 1.45 to 1.75 V as the number of methylene groups (chain length) increases in the imine compartment [30]. As the ring size increases due to flexibility, the planarity of the complex decreases and the oxidation is more difficult. Ring size and rigidity of the ligand environment influence structural and electrochemical properties of the complexes.

3.3. *Kinetic studies of hydrolysis of 4-nitrophenylphosphate*

The catalytic activity of the nickel(II) complexes on hydrolysis of 4-nitrophenylphosphate was investigated spectrophotometrically by the absorption increase at 420 nm due to formation of 4-nitrophenolate over time intervals of 5 min in DMF at 25 °C. Solution of the complexes (10^{-3} M dm^{-3}) in DMF were treated with 100 equivalents (10^{-1} M dm^{-3}) of 4-nitrophenylphosphate in air. Time-dependent formations of 4-nitrophenolate in the presence of complexes are shown in figure 1. The rate of hydrolysis of 4-nitrophenyl phosphate for Ni_2L^5 (9.84×10^{-3} min^{-1}) was the highest and that for Ni_2L^1 (6.35×10^{-3} min^{-1}) was the lowest. These values are comparable to constants reported by Yamaguchi *et al.* for hydrolytic cleavage of 4-NPP by binuclear Ni(II) complexes [31]. The observed initial rate constants for the nickel(II) complexes are given in table 2. Catalytic activity of the complexes increase as the macrocyclic ring size increases [32–34], because intrinsic flexibility of the complexes makes the metal ion reduce easily and binds with the substrate. The formation of 4-nitrophenolate requires the presence of two metal ions in close proximity. Hence, the initial rate values of binuclear complexes are comparatively high [31].

3.4. *Antimicrobial and antifungal studies*

Antibacterial activities of all complexes were tested by the well-diffusion method using nutrient agar against bacteria such as *Staphylococcus aureus (ATCC 25923)*, *Bacillus cereus (ATCC 6633)*, *Escherichia coli (ATCC 35218)*, *Klebsiella pneumonia (ATCC*

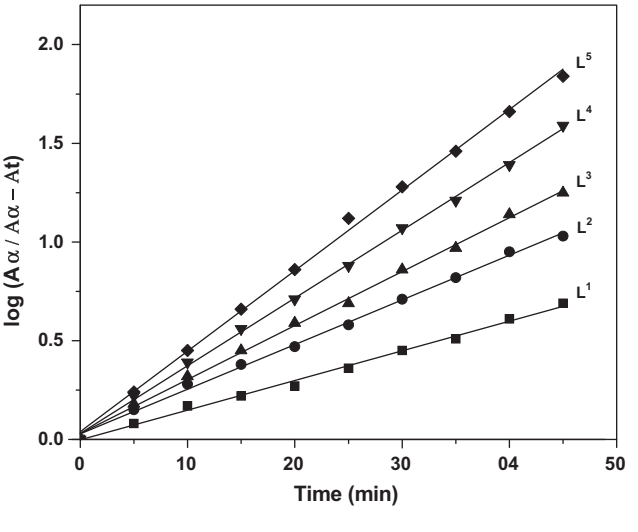

Figure 1. Hydrolysis of 4-nitrophenylphosphate by binuclear nickel(II) complexes.

27736), *Streptococcus mutans (ATCC 25175)*, and *Pseudomonas aeruginosa (ATCC 2036)* and the antifungal activities of the complexes were tested by using sabouraud dextrose agar against human pathogenic fungus *C. albicans (ATCC 90028)*. The radial growth of the colony was recorded on completion of the incubation and the mean diameter for each complex at a concentration of 1 mg mL^{-1} was recorded [35].

The screening results of complexes are shown in table 3. All complexes efficiently inhibit growth of the bacteria and fungus. $Ni_2L^{4\text{ and }5}$ show higher activity against the bacteria and fungus except *P. aeruginosa* and *S. aureus*, respectively. Ni_2L^1 and Ni_2L^2 show lowest activity against the bacteria and fungus. Ni_2L^3 show moderate activity against the bacteria and fungus except *S. mutans* and *P. aeruginosa*. The trends in antimicrobial activity may be due to the structures and position of the ligand in the complexes.

The tested complexes show activity comparable with N-substituted tetraazamacrocycles reported in the literature [36]. This antimicrobial activity of nickel(II) complexes may be due to structures of the ligands which make the nickel(II) complexes potent bacteriostatic agents. The variation in the activity of the complexes against different organisms depend either on the impermeability of the cell of the microbes or difference in ribosome of microbial cells [37].

3.5. *DNA binding studies*

3.5.1. Electronic absorption titration. Interaction of Ni_2L^1 with calf thymus DNA (CT DNA) has been investigated by using absorption spectra. Intense absorption with maximum of 255 nm for Ni_2L^1 was attributed to intra-ligand π–π^* transition. Absorption spectra of the nickel(II) complex in the absence and presence of CT DNA are given in figure 2. The complex binds to DNA through intercalation causing hypsochromism. A similar hypsochromism has been observed for a Ni(II) complex bearing N–H and bromo groups [38]. To compare quantitatively the binding strength of the complexes, the intrinsic binding constants K_b of the complexes with CT–DNA were determined according to the following equation [39]:

Table 3. Antimicrobial properties of binuclear nickel(II) complexes.

	Zone of Inhibition (mm) 100 μg ml^{-1}						
	Ni_2L^1	Ni_2L^2	Ni_2L^3	Ni_2L^4	Ni_2L^5	A	T
Test Bacteria							
S.a	15 ± 0.1	12 ± 0.2	13 ± 0.1	23 ± 0.1	–	31	20
B.c	12 ± 0.1	12 ± 0.1	14 ± 0.1	21 ± 0.1	23 ± 0.1	28	7
E.c	12 ± 0.1	11 ± 0.1	11 ± 0.2	16 ± 0.1	19 ± 0.2	NT	8
K.p	15 ± 0.1	16 ± 0.1	14 ± 0.2	17 ± 0.2	20 ± 0.2	NT	5
S.m	11 ± 0.1	13 ± 0.2	–	14 ± 0.2	16 ± 0.2	NT	12
P.a	12 ± 0.1	11 ± 0.1	–		11 ± 0.1	NT	8
Test Fungus							
C.a	15 ± 0.1	13 ± 0.1	13 ± 0.1	17 ± 0.1	17 ± 0.2	NT	–

Notes: *S.a*: *Staphylococcus aureus (ATCC 25923)*, *B.c*: *Bacillus cereus (ATCC 6633)*, *E.c*: *Escherichia coli (ATCC 35218)*, *K.p*: *Klebsiella pneumonia (ATCC 27736)*, *S.m*: *Streptococcus mutans (ATCC 25175)*, *P.a*: *Pseudomonas aeruginosa (ATCC 2036)*, *C.a*: *Candida albicans (ATCC 90028)*, A: Ampicillin (10 μg), T: Tetracycline (30 μg), (NT): not tested, (–): no inhibition.

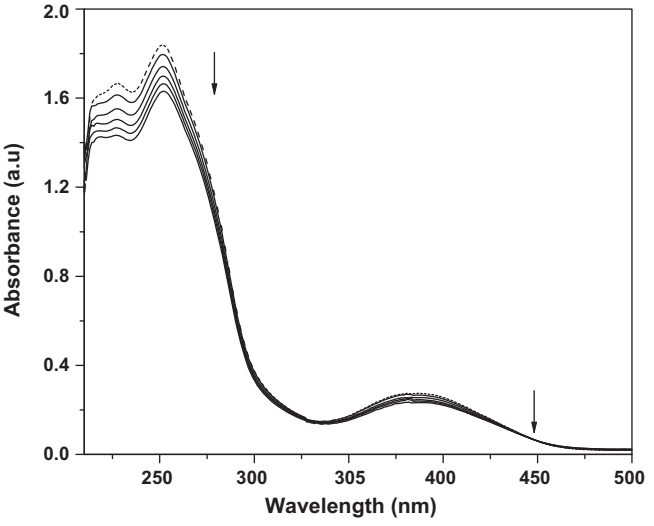

Figure 2. Electronic spectra of Ni_2L^1 (30 μM) in the presence of increasing amounts of CT DNA; [DNA] = 0–50 μM. The arrow indicates the absorbance changes upon increasing DNA concentration.

$$[\mathrm{DNA}]/(\varepsilon_a - \varepsilon_f) = [\mathrm{DNA}]/(\varepsilon_b - \varepsilon_f) + 1/K - b(\varepsilon_b - \varepsilon_f)$$

where, [DNA] is the concentration of DNA in base pairs, the apparent absorption coefficients ε_a, ε_f, and ε_b correspond to A_{obsd}/[complex], the extinction coefficient for the free complexes, and the extinction coefficient for the complexes in the fully bound form, respectively. In plots of DNA] / ($\varepsilon_b - \varepsilon_f$) *versus* [DNA], K_b is given by the ratio of the slope to the intercept. The intrinsic binding constant K_b of Ni_2L^1 is $2.80 \times 10^5\,M^{-1}$. It is likely that binding of Ni_2L^1 attributed to cyclam is from formation of several hydrogen bonds between –NH– in cyclam and base pairs in DNA [40–42]. The introduction of side chain containing polyaza groups could enhance binding to DNA. These spectral characteristics suggest that our complexes interact with DNA through a mode that involves interaction between the aromatic chromophore and base pairs of DNA.

3.5.2. Fluorescence spectra. The nickel(II) complex binds to CT DNA via intercalation as given through emission quenching. Ethidium bromide is a fluorescent probe for DNA structure and has been employed in examinations of the mode of metal complex binding to DNA. To investigate the interaction of Ni_2L^1 with DNA, fluorescence emission titration analyzes were undertaken. The spectra of complex in the absence and presence of calf thymus CT DNA are shown in figure 3. Fluorescence intensities at 601 nm (510 nm excitation) were measured at different complex concentrations. Addition of complex showed reduction in the emission intensity. The reduction of emission intensity gives a measure of the DNA binding propensity of the complex and stacking interaction (intercalation) between the adjacent DNA base pairs [43]. The quenching of EB bound to DNA by complex is in agreement with the linear Stern–Volmer equation.

$$I_0/I = 1 + K_{SV}[Q]$$

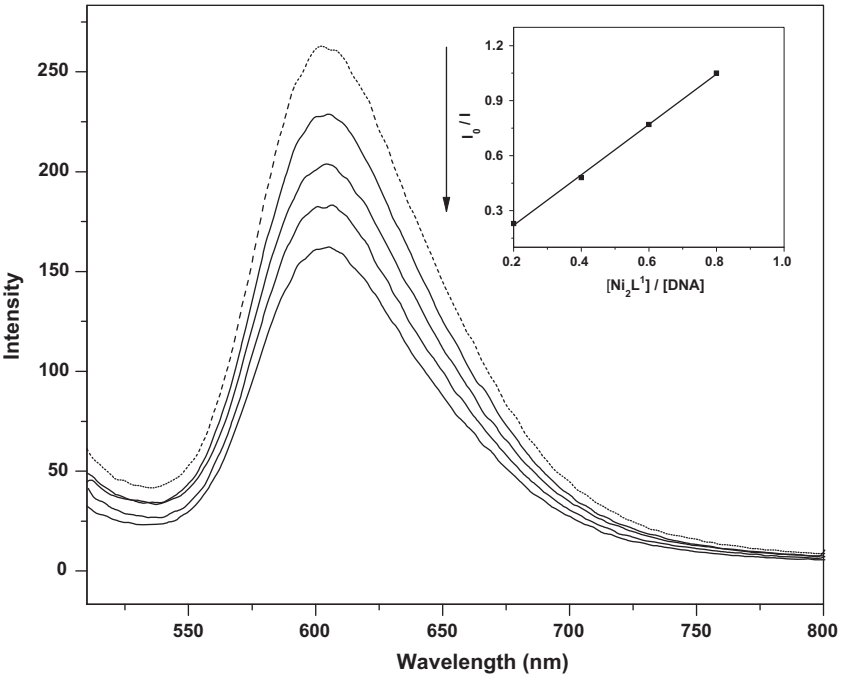

Figure 3. Emission spectra of the DNA–EB system (20 μM and 0.33 μM), $\lambda_{max} = 500$ nm, $\lambda_{emi} = 510$–650 nm, in the presence of 0–40 μM Ni_2L^1. The arrow indicates the emission intensity changes upon increasing complex concentration. Inset: Plot of I_0/I *vs.* Ni_2L^1 for titration of Ni_2L^1 to CT DNA–EB system.

Linear fit of I_0/I *versus* [complex]/[DNA], K_{sv} is given by the ratio of the slope to intercept. I_0 is the emission intensity of EB–DNA in the absence of complex; I is the emission intensity of EB–DNA in the presence of complex; and Q is the concentration of quencher, by taking a CT DNA binding constant of $1.0 \times 10^7\,M^{-1}$ for EB, an apparent DNA binding constant of $2.00 \times 10^6\,M^{-1}$ was derived for Ni_2L^1. The K_{sv} values imply that the complex can strongly interact with DNA.

3.6. *DNA cleavage studies*

In order to assess the cleavage of DNA by the nickel(II) complex, agarose gel electrophoresis has been performed with the supercoiled form of plasmid DNA. Supercoiled pBR322 DNA (0.5 μg) in the presence of Ni_2L^1 was carried out in a medium of 50 mM Tris-HCl/1 mM NaCl Buffer (pH 7.5). Supplementary Material exhibits the concentration dependence of the cleavage reactions. Form I (Super coiled DNA) was converted to Form II (Nicked Circular DNA) at 100 μM of the complex. As the concentration was further increased, appearance of Form III (linear form of the DNA) was also observed. The cleavage efficiency was 32.55% at 100 μM and increased to 50.40% at 200 μM, with 3.70% and 17.35% of the DNA completely cleaved to Form III (linear) for 100 and 200 μM. Complexes of polyamine ligands play an important role due to their good nuclease activity [44]. The experiments indicate that complex has the ability to cleave super-coiled DNA without reducing agent or light. The cleavage ability might be due to binding affinity of the complex to the DNA.

4. Conclusion

We have synthesized and characterized five binuclear Ni(II) complexes. The complexes have been screened for activity against bacteria and a fungus. Electronic absorption and fluorescence spectra measurements indicate strong binding with CT DNA, presumably via intercalation. Catalytic activity increases due to increase of methylene groups around the metal. Variations in chain length of the imine compartment of the complexes influence spectral, electrochemical, and catalytic properties of the nickel(II) complexes.

Acknowledgment

Financial support from University Grants Commission, New Delhi, is gratefully acknowledged.

References

[1] S. Brooker, G.B. Caygill, P.D. Croucher, T.C. Davidson, D.L.J. Clive, S.R. Magnuson, S.P. Cramercd, C.Y. Ralston. *J. Chem. Soc., Dalton Trans*., 3113 (2000).
[2] T. Chattopadhyay, K.S. Banu, A. Banerjee, J. Ribas, A. Majee, D. Das. *J. Mol. Struct.,* **833**, 13 (2007).
[3] M. Halma, A. Bail, F. Wypych, S. Nakagaki. *J. Mol. Catal. A: Chem.,* **243**, 44 (2006).
[4] W.A. Wolkert, T.J. Hoffman. *Chem. Rev.,* **99**, 2269 (1999).
[5] M. Meyer, V. Dahaoui-Gindrey, C. Lecomte, R. Guilard. *Coord. Chem. Rev.,* **180**, 1313 (1998).
[6] P. Caravan. *Chem. Soc. Rev.,* **35**, 512 (2006).
[7] X. Liang, P.J. Sadler. *Chem. Soc. Rev.,* **33**, 246 (2004).
[8] M.S. Ray, S. Chattopadhyay, M.G.P. Drew, A. Figuerola, J. Ribas, A. Ghosh. *Eur. J. Inorg. Chem.,* **4562**, (2005).
[9] L. Small, R. Schmidt. *Chem. Eur. J.,* **10**, 1014 (2004).
[10] P.R. Reddy, K.S. Rao. *Chem. Biodivers,* **3**, 231 (2006).
[11] C.J. Burrows, S. Rokita. *Acc. Chem. Res.,* **27**, 295 (1994).
[12] J.G. Muller, X. Chen, A.C. Dadiz, S.E. Rokita, C.J. Burrows. *J. Am. Chem. Soc.,* **114**, 6407 (1992).
[13] X. Chen, C.J. Burrows, S.E. Rokita. *J. Am. Chem. Soc.,* **114**, 322 (1992).
[14] D.P. Mack, P.B. Dervan. *J. Am. Chem. Soc.,* **112**, 4604 (1990).
[15] H.Y. Wang, W.B. Yuan, Q. Zhang, S.W. Chen, S.S Wu. *Transition Met. Chem.,* **33**, 593 (2008).
[16] N. Sengottuvelan, J. Manonmani, M. Kandaswamy. *Polyhedron,* **21**, 2767 (2002).
[17] R. Prabu, A. Vijayaraj, R. Suresh, R. Shenbhagaraman, V. Kaviyarasan, V. Narayanan. *Spectrochim. Acta, Part A,* **78**, 601 (2011).
[18] Q. Wang, C. Wilson, F. Alexander, J. Blake, Simon, R. Collinson, A. Peter, M. Schrodera. *Tetrahedron Lett.,* **47**, 8983 (2006).
[19] G. Royal, V.D. Gindrey, S. Dahaowi, A. Tabard, R. Guilard, C. Lecomte. *Eur. J. Org. Chem.,* **9**, 1971 (1998).
[20] D. Gayathri, D. Velmurugan, K. Ravikumar, S. Sreedaran, V. Narayanan. *Acta Cystallogr., Sect. E*, **62**, 3714 (2006).
[21] J. Marmur. *J. Mol. Biol.,* **3**, 208 (1961).
[22] S. Sreedaran, K.S. Bharathi, A.K. Rahiman, K. Rajesh, G. Nirmala, V. Narayanan. *J. Coord. Chem.,* **61**, 3594 (2008).
[23] J. Geary. *Coord. Chem. Rev.,* **7**, 81 (1971).
[24] G. Das, R. Shukla, S. Mandal, R. Singh, P.K. Bharadwaj, K.H. Whitmire. *Inorg. Chem.,* **36**, 323 (1997).
[25] M. Lachkar, R. Guilard, A. Attamani, A. De Clan, J. Fisher, R. Weiss. *Inorg. Chem.,* **37**, 1575 (1998).
[26] K.R. Adam, G. Andereg, L.F. Lindoy, H.C. Lip, M. Mcpartlin, J.H. Rea, P.J. Tasker. *Inorg. Chem.,* **19**, 2956 (1980).
[27] S.K. Mandal, B. Adhikary, K. Nag. *J. Chem. Soc., Dalton Trans*., 1175 (1986).
[28] B. Srinivas, N. Arulsamy, P.S. Zacharias. *Polyhedron,* **10**, 731 (1991).
[29] D. Volkmer, B. Hommerich, K. Griesar, W. Haase, B. Krebs. *Inorg. Chem.,* **35**, 3792 (1996).
[30] M. Thirumavalavan, P. Akilan, M. Kandaswamy. *Supramol. Chem.,* **16**, 495 (2004).
[31] K. Yamaguchi, F. Akagi, S. Fujinami, M. Suzuki, M. Shionoya, S. Suzuki. *Chem. Commun.,* **375**, (2001).
[32] N. Sengottuvelan, D. Saravanakumar, M. Kandaswamy. *Polyhedron,* **26**, 3825 (2007).

[33] Z. Puterova, J. Valentova, Z. Bojkova, J. Kozısek, F. Devınsky. *J. Chem. Soc., Dalton Trans*., 1484 (2011).
[34] M. Thirumavalavan, P. Akilan, M. Kandaswamy. *Polyhedron,* **24**, 1781 (2005).
[35] D.G. McCollum, C. Fraser, R. Ostrander, A.L. Rheingold, B. Bosnich. *Inorg. Chem.,* **33**, 2383 (1994).
[36] S.M. Emam, F.A. El-Saied, S.A. Abou El-Enein, H.A. El-Shater. *Spectrochim. Acta, Part A,* **72**, 291 (2009).
[37] T.G. Roy, S.K.S. Hazari, B.K. Dey, H.A. Miah, C. Bader, D. Rehder. *Eur. J. Inorg. Chem.,* **4115**, (2004).
[38] H.G. Diaz, A.S. González, Y.G. Díaz. *J. Inorg. Biochem.,* **100**, 1290 (2006).
[39] A.M. Pyle, J.P. Rehmann, R. Meshoyrer, C.V. Kumar, N.J. Turro, J.K. Barton. *J. Am. Chem. Soc.,* **111**, 3051 (1989).
[40] Y.U. Huang, Q.S. Lu, J.I. Zhang, Z.W. Zhang, Y.U. Zhang, S.Y. Chen, L.I. Kun, X.Y. Tan, H.Q. Yua. *Bioorg. Med. Chem.,* **16**, 1103 (2008).
[41] N. Raman, K. Pothiraj, T. Baskaran. *J. Coord. Chem.,* **64**, 3900 (2011).
[42] N. Raman, K. Pothiraj, T. Baskaran. *J. Coord. Chem.,* **64**, 4286 (2011).
[43] J.B. Lepecq, C. Paoletti. *J. Mol. Biol*., **l27**, 87 (1967).
[44] Q.L. Li, J. Huang, Q. Wang, N. Jiang, C.Q. Xia, H.H. Lin, X.Q. Yu. *Bioorg. Med. Chem.,* **14**, 4151 (2006).